CrossMark

BREAST

Discrimination between benign and malignant breast lesions using volumetric quantitative dynamic contrast-enhanced MR imaging

Ziliang Cheng[1,2] · Zhuo Wu[1,2] · Guangzi Shi[1] · Zhilong Yi[1] · Mingwei Xie[1] · Weike Zeng[1] · Chao Song[1] · Chushan Zheng[1] · Jun Shen[1,2]

Abstract

Objective To determine the diagnostic performance of volumetric quantitative dynamic contrast-enhanced MRI (qDCE-MRI) in differentiation between malignant and benign breast lesions.

Methods DCE-MRI was performed in 124 patients with 136 breast lesions. Quantitative pharmacokinetic parameters K^{trans}, K_{ep}, V_e, V_p and semi-quantitative parameters TTP, MaxCon, MaxSlope, AUC were obtained by using a two-compartment extended Tofts model and three-dimensional volume of interest. Morphologic features (lesion size, margin, internal enhancement pattern) and time-signal intensity curve (TIC) type were also assessed. Logistic regression analysis was used to determine predictors of malignancy, followed by receiver operating characteristics (ROC) analysis to evaluate the diagnostic performance.

Results qDCE parameters (K^{trans}, K_{ep}, V_p, TTP, MaxCon, MaxSlope and AUC), morphological parameters and TIC type were significantly different between malignant and benign lesions ($P \leq 0.001$). Multivariate logistic regression analyses showed that K^{trans}, K_{ep}, MaxSlope, size, margin and TIC type were independent predictors of malignancy. The diagnostic accuracy of logistic models based on qDCE parameters alone, morphological features plus TIC type, and all parameters combined was 94.9%, 89.0%, and 95.6% respectively.

Conclusion qDCE-MRI can be used to improve diagnostic differentiation between benign and malignant breast lesions in relation to morphology and kinetic analysis.

Key Points
- qDCE-MRI parameters are useful for discriminating between malignant and benign breast lesions.
- K^{trans}, K_{ep} and MaxSlope were independent predictors of breast malignancy.
- qDCE-MRI has a better diagnostic ability than morphology and kinetic analysis.
- qDCE-MRI can be used to improve the diagnostic accuracy of breast malignancy.

Keywords Breast · Neoplasms · Magnetic resonance imaging · Dynamic contrast-enhanced MRI · Diagnosis

Ziliang Cheng and Zhuo Wu contributed equally to this work

✉ Jun Shen
   shenjun@mail.sysu.edu.cn

[1] Department of Radiology, Sun Yat-Sen Memorial Hospital, Sun Yat-Sen University, No. 107 Yanjiang Road West, Guangzhou, Guangdong 510120, China

[2] Guangdong Provincial Key Laboratory of Malignant Tumour Epigenetics and Gene Regulation, Medical Research Centre, Sun Yat-Sen Memorial Hospital, Sun Yat-Sen University, Guangzhou 510120, China

Abbreviations

qDCE-MRI	quantitative dynamic contrast-enhanced magnetic resonance imaging
K^{trans}	volume transfer constant
K_{ep}	reverse reflux rate constant
EES	extravascular extracellular space
V_e	volume fraction of EES
V_p	volume fraction of plasma
TTP	time to peak
MaxCon	maximum concentration
MaxSlope	maximum slope
AUC	area under curve
ROC	receiver operating characteristic

AUROC	area under receiver operating characteristic curve
PPV	positive predictive value
NPV	negative predictive value
TIC	time-signal intensity curve
3D-VOI	three-dimensional volume of interest
T1W-VIBE	T1-weighted volume interpolated body examination
ROI	region of interest
ICC	intra-class correlation coefficient
OR	odds ratio
CI	confidence interval

Introduction

Breast cancer is one of the most common malignancies and the second leading cause of cancer death among women [1]. MR imaging (MRI) is not only helpful in screening but also in defining the primary tumour. It is also better than other methods in assessing the response to chemotherapy treatment [2]. The main advantage of MRI over mammography or ultrasonography is its higher sensitivity [3, 4]. It can detect cancers missed by mammography or ultrasound in women who have dense breasts and can influence the surgical staging of breast cancer by enabling identification of multifocal and multicentric cancers in the ipsilateral and/or contralateral breast [5]. Conventional breast MRI includes morphological assessment, enhancement and time signal intensity curve (TIC) analysis [6–9]. Quantitative dynamic contrast-enhanced MRI (qDCE-MRI) is promising, because it can provide multiple pharmacokinetic parameters including semi-quantitative parameters (model-free parameters) and quantitative parameters (model-based parameters derived from pharmacokinetic model calculation), which can fundamentally describe the tumour vascularity and permeability. Previously, qDCE-MRI has been shown to improve the diagnostic specificity of MRI in many cancers [10–13]. Compared with semi-quantitative parameters, quantitative parameters are less affected by a wide variability in MRI scanners, scanning sequence, temporal resolution, injection of contrast media, and image post-processing calculation [14–16]. To ensure the repeatability and reproducibility of the parameter calculation, three fundamental entities are required for qDCE-MRI: (1) Pre-contrast T1 mapping to convert signal intensity into contrast agent concentration, (2) measurements based on both arterial input function and regions of interest tissue, and (3) a suitable pharmacokinetic model to analyse such data [17]. Nonetheless, the use of qDCE-MRI in differentiation between benign and malignant breast lesions has not been well evaluated. Previous studies on qDCE-MRI in breast cancer differed widely in terms of temporal resolution and sampling duration

of data acquisition, and pharmacokinetic models used for calculation, and had a limited number of included patients [18–20].

In this study, we aimed to find if and which pharmacokinetic parameters derived from DCE data using a two-compartment extended Tofts model and three-dimensional volume of interest (3D-VOI) would be suitable for the differentiation between malignant and benign breast lesions. Furthermore, we assessed the specificity of the found parameters.

Materials and Methods

Patients

Between April 2016 and July 2016, 180 consecutive patients who were suspected to have solid breast tumour on mammography and ultrasound examination were enrolled. The study was approved by the institutional review board of Sun Yat-Sen Memorial Hospital of Sun Yat-Sen University. Written informed consent was obtained from all patients. All patients underwent biopsy before MRI examination. All patients with histopathologically proven malignant lesions underwent surgery as well as the patients with high-risk lesions including papilloma, radial scars and benign phyllodes tumour. Patients were excluded if they underwent neoadjuvant chemotherapy, or if have had a recent surgical procedure in the breast before the MRI examination. Three patients with obvious motion artefacts on MRI were also excluded. Finally, 124 female patients, aged from 25-74 years with a mean of 47.6±11.9 years, were included in this study.

MRI

DCE-MRI was performed on a 1.5 T unit (Magnetom Avanto; Siemens Medical Solutions, Erlangen, Germany). The body coil was used as the transmitter, and an 8-channel phased-array breast coil (Siemens Medical Solutions, Erlangen, Germany) was used as the receiver. For all pre-menopausal women, the examination was performed between the seventh and 14th day of the menstrual cycle to reduce hormonal variations and minimize the enhancement on the fibroglandular tissue. The patients were placed in the prone position with their breasts placed in a holder to reduce motion. The acquisition sequences included T1- and T2-weighted imaging, and DCE imaging. After axial and sagittal T2-weighted imaging using inversion recovery for fat-suppression (repetition time/echo time [TR/TE], 3920/68 ms; inversion time, 170 ms; flip angle, 150°; field of view [FOV], 350×350 mm^2; voxel size, 0.5×0.5×5.0 mm^3;section thickness/gap, 5.00/0 mm) and Dixon T1-weighted imaging (TR/TE, 6.86/2.39 ms; flip angle, 15°; FOV, 360×360 mm^2; voxel size, 0.9×0.9×2.0 mm^3,

section thickness, 2.00 mm and overlapping gap, 0.1 mm) were obtained, axial DCE imaging was acquired by using a 3D T1-weighted volume interpolated body examination (T1W-VIBE) sequence (TR/TE, 4.87/2.4 ms; flip angle, 10°; FOV, 380×380 mm^2; voxel size, 0.5×0.5×3.0 mm^3; slice thickness, 3.00 mm and overlapping gap, 1.5 mm). The DCE acquisition consisted of 40 measurements with a temporal resolution of 8 sec. After the initial two dynamic measurements, Gd-DTPA-BMA (Omniscan, GE Healthcare, Ireland) at the dosage of 0.1 mmol/kg was administered by intravenous bolus injection using an MR-compatible power injector (Spectris, Medrad, Pittsburgh, PA) at a flow rate of 3.5ml/ sec, followed by a 20 ml saline flush. Before DCE acquisition, multiple flip angle images (2°, 4°, 6°, 8°, 10° and 12°) were obtained for the calculation of T1 maps using the same sequence and parameters except for the flip angle.

Image analysis

The morphology (size, margin and internal enhancement pattern) and time-signal intensity curve (TIC) of the lesions were assessed in isolation, and in a blinded manner by one radiologist (J.S. with 5 years of experience with DCE-MRI). The size was measured in the greatest diameter in either transverse or sagittal planes. The margin was categorised as smooth, irregular, or spiculated; and the internal enhancement pattern was categorised as homogeneous, heterogeneous or rim [19]. The TIC types were categorised as persistent enhancing (type I), plateau (type II) or washout (type III) according to the previously reported method [19].

DCE-MRI data were transferred to an off-line workstation and analysed by using a specialized quantitative analysis software (Omni Kinetics, GE Healthcare). Before parameter calculation, a nonlinear registration framework utilising the Free Form Deformation algorithm was used to correct misalignment caused by body motion between consecutive DCE scans, and the signal intensity was converted into gadolinium concentration using the variable flip angle method [17, 21]. Patient-specific arterial input function was drawn on the thoracic aorta. A two-compartment extended Tofts model was used to obtain quantitative parameters. To obtain perfusion parameters in a 3D-VOI, regions of interest (ROIs) were manually drawn on each slice to cover the whole lesion. DCE-MRI data were analysed by two radiologists (Z.W., and Z.C. with 5 years and 3 years of experience with breast MRI), who were blinded for histology. Necrotic or cystic areas of the lesions, if presented, were excluded from the evaluation. Quantitative parameters including K^{trans} (volume transfer constant), K_{ep} (reverse reflux rate constant), V_e (volume fraction of extravascular extracellular space), and V_p (volume fraction of plasma), and semi-quantitative parameters including TTP (time to peak), MaxCon (maximum concentration), MaxSlope (maximal slope) and AUC (area under curve), were

calculated. The detailed calculation of the extended Tofts model has been reported previously [22–24].

Statistical analysis

The agreement of the evaluation of qDCE-MRI parameters between the two readers was calculated using the intra-class correlation coefficient (ICC). An ICC value >0.75 represents well to excellent agreement, and a value between 0.4 and 0.75 represents fair to moderate agreement. Data from the two readers were averaged for analysis. The normality of distribution of qDCE-MRI parameters was determined by using the Shapiro-Wilk test. All numerical data were presented as mean ± standard deviation. The Mann-Whitney U test and χ^2 test were respectively used to compare the numerical and categorical variables between benign and malignant lesions. Univariate binary logistic regression analysis was used to determine if a single parameter was able to differentiate between malignant and benign lesions. Receiver operating characteristics (ROC) analysis was used to evaluate the diagnostic ability of the parameters. The area under the ROC curve (AUROC), sensitivity, specificity, positive predictive value (PPV), negative predictive value (NPV) and accuracy were calculated for each parameter and the optimal threshold was determined by the Youden index. Those variables with p value less than 0.05, as determined by the univariate binary logistic regression analysis or by χ^2 test, were chosen for multivariate binary logistic regression analysis to determine the parameters that can best predict the diagnosis of malignancy. A collinearity diagnosis was made on the logistic regression model to test the independence of predictors. If there was multicollinearity, a least absolute shrinkage and selection operator (LASSO) model was used to select the potential predictors to be used by shrinking the coefficients toward zero through setting a constraint on the sum of the absolute standardized coefficients. Then, multivariate binary logistic regression analyses were performed to generate the coefficients of all independent predictors from LASSO selection. Odds ratios (OR) as estimates of relative risk with 95% confidence intervals (CI) were obtained for each independent predictor. For multivariate logistic regression, three models were developed: model 1 in which qDCE parameters were chosen as the independent risk factors; model 2 in which morphological parameters and TIC type were chosen as the independent risk factors; model 3 in which qDCE parameters, morphological parameters and TIC type were chosen as the independent risk factors. The diagnostic performance of three models was evaluated by ROC analysis and their AUROCs were compared by using the Hanley and McNeill test. The sensitivity, specificity, PPV, NPV and accuracy were calculated for each model. A two-sided p value of less than 0.05 was considered to indicate a significant difference. All statistical tests were performed by

using R3.1.1 (www.r-project.org) and SPSS (version 21.0; SPSS, Chicago, Ill, USA).

Results

Study population

There was a total of 136 lesions in the 124 patients, including 105 malignant lesions and 31 benign lesions. 83 of 105 malignant lesions were diagnosed as infiltrating ductal carcinomas (IDC), eight were diagnosed as ductal carcinomas in situ (DCIS), four were diagnosed as infiltrating lobular carcinomas (ILC), six were diagnosed as papillary carcinomas, one was diagnosed as carcinosarcoma, one was diagnosed as adenoid cystic carcinoma (ACC), and two were diagnosed as mucinous carcinomas. Twenty-one of 31 benign lesions were diagnosed as fibroadenomas (FA), three were diagnosed as papillomas, five were diagnosed as radial scars, and two were diagnosed as benign phyllodes tumours.

Morphology and TIC

The averages of lesion size, margin, internal enhancement pattern and TIC, and the comparison between malignant and benign lesions are shown in Table 1. The malignant lesions had a greater size than the benign lesions. Smooth margin, homogeneous enhancement and type I TIC were more often found in the benign lesions (Fig. 1A), while irregular or spiculated margin, heterogeneous or rim enhancement, and type II or III TICs were predominant features of the malignant lesions (Fig. 2A). ROCs of each parameter are shown in Fig. 3A. The diagnostic performance of these parameters for discrimination between malignant and benign breast lesions is shown in Table 2. TIC type had the highest accuracy of 0.890 for the diagnosis of malignancy.

qDCE-MRI parameters

The ICC of qDCE parameters between the two readers was 0.862 for K^{trans} (95% CI: 0.809-0.900), 0.836 for K_{ep} (95% CI: 0.778-0.880), 0.901 for V_e (95% CI: 0.864-0.929), 0.988 for V_p (95% CI: 0.983-0.991), 0.897 for TTP (95% CI: 0.858-0.925), 0.707 for MaxCon (95% CI: 0.590-0.791), 0.782 for MaxSlope (95% CI: 0.705-0.840), and 0.730 for AUC (95% CI: 0.631-0.805). Therefore, the agreement between the two readers in the evaluation of the qDCE parameters was good.

The averages of the qDCE parameters and their comparison between malignant and benign lesions are shown in Table 1. The mean K^{trans}, K_{ep}, V_p, MaxCon, MaxSlope and AUC values were significantly higher in malignant lesions than those in benign lesions ($p \leq 0.001$). The mean TTP in malignant lesions was significantly lower than that in benign

Table 1 Morphological parameters, TIC types and DCE-MRI parameters for malignant and benign breast lesions ($n = 136$)

Parameters	Benign (n=31)	Malignant (n=105)	p value
Size (mm) [a]	14.9±9.9 (range 4-42)	27.5±13.8 (range 6-84)	<0.001[#]
Margin			<0.001[*]
Smooth[b]	14 (45.2%)	7 (6.7%)	
Irregular[b]	17 (54.8%)	65 (61.9%)	
Spiculated[b]	0 (0)	33 (31.4%)	
Enhancement			<0.001[*]
Homogeneous[b]	13 (41.9%)	11 (10.5%)	
Heterogeneous[b]	17 (54.8%)	75 (71.4%)	
Rim[b]	1 (3.2%)	19 (18.1%)	
TIC type			<0.001[*]
Type I[b]	18 (58.1%)	2 (1.9%)	
Type II[b]	12 (38.7%)	55 (52.3%)	
Type III[b]	1 (3.2%)	48 (45.7%)	
K^{trans} (min^{-1})[a]	0.0336±0.0150	0.1215±0.1093	<0.001[#]
K_{ep} (min^{-1})[a]	0.2968±0.1521	0.8782±0.4300	<0.001[#]
V_e[a]	0.1404±0.0458	0.1372±0.0537	0.726[#]
V_p[a]	0.0030±0.0036	0.0153±0.0127	<0.001[#]
TTP (min)[a]	5.4597±0.6422	3.6430±1.0317	<0.001[#]
MaxCon[a]	0.1032±0.0280	0.1461±0.0519	0.001[#]
MaxSlope[a]	0.1106±0.0520	0.2595±0.0978	<0.001[#]
AUC[a]	0.4448±0.1547	0.7138±0.2663	<0.001[#]

TIC time-signal intensity curve; # Mann-Whitney U test; * χ^2 test. [a] Data are mean±SD. [b] Data are number of lesions, with percentage in parentheses

lesions (p<0.001). There was no significant difference in the V_e value between malignant and benign breast lesions (p=0.726) (Fig. 1B, C and 2B, C). ROCs of each parameter are shown in Fig. 3B, C. The diagnostic performances of these parameters are shown in Table 2. K^{trans} had the highest specificity of 0.935 and highest accuracy of 0.890 for diagnosis of malignancy.

Multivariate binary logistic regression analysis

K^{trans}, K_{ep}, and MaxSlope were independent predictors for malignancy in model 1, as determined by univariate analysis, collinearity diagnosis, LASSO selection and multivariate analysis. For model 2, the lesion size, margin and TIC were independent predictors for malignancy. For model 3, the lesion size, margin, TIC, K^{trans} and MaxSlope were independent predictors for malignancy. The diagnostic performance of the three models is shown in Table 3. Model 3 had the highest diagnostic accuracy among the three models. ROCs of the three models are shown in Fig. 3D. There was a significant difference in the AUROC between model 2 and model 3 (p=0.006), while no difference was found between model 1
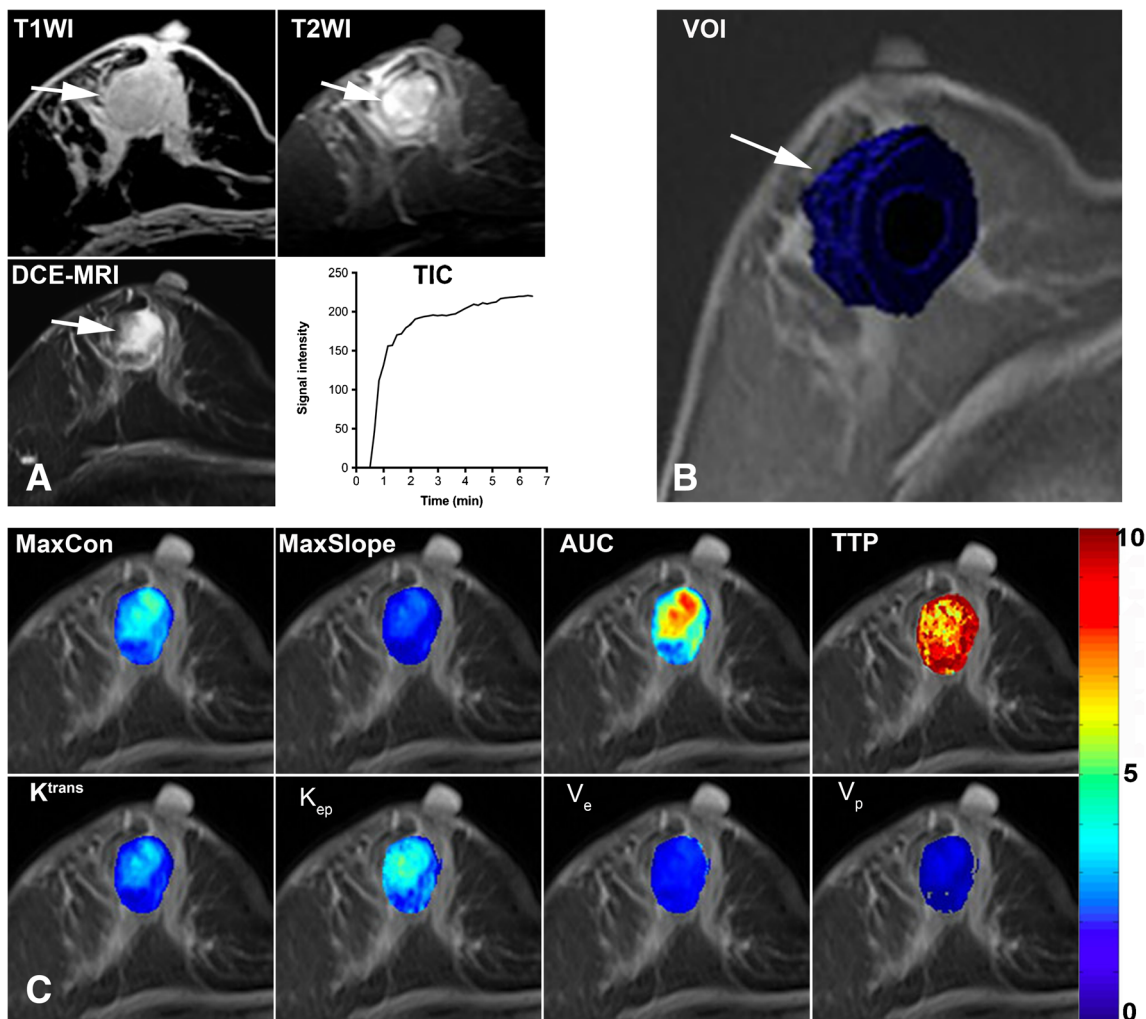
Fig. 1 Benign breast tumour. (**A**) A 35-year-old woman has a benign phyllodes tumour in the right breast, which is seen as a 27-mm mass (arrows) with hypointense signal on T1WI and hyperintense signal on fat-suppressed T2WI, with a smooth margin and heterogeneous enhancement on DCE-MRI (2 min after contrast injection) and a time-signal intensity curve (TIC) of type I; (**B**) DCE-MRI parameters are evaluated by a 3-D volume of interest (arrow); (**C**) Pseudo-colorized maps show individual parameters derived from DCE-MRI. This tumour has low MaxCon (0.1253), MaxSlope (0.1573), AUC (0.6175), K^{trans} (0.0192 min^{-1}), K_{ep} (0.1976 min^{-1}), V_e (0.0976) and V_p (0.0070), but high TTP (5.6178 min).

and model 2 ($p>0.05$), as determined by the Hanley and McNeill test.

Discussion

In this study, we used a 3-D-VOI and a two-compartment extended Tofts model to derive qDCE parameters of breast lesions. Our results showed that K^{trans}, K_{ep}, V_p, MaxCon, MaxSlope, TTP and AUC of malignant lesions were different from those of benign lesions. The multivariate binary logistic regression analysis showed that K^{trans}, K_{ep} and MaxSlope were independent predictors of malignancy. The logistic model including these three parameters combined with lesion size, margin and TIC had a higher diagnostic accuracy than the logistic model including only lesion size, margin and TIC for the discrimination of malignant from benign breast lesions. Therefore, the diagnostic performance was improved when morphological parameters and TIC were combined with qDCE parameters.

To date, only a few studies have used 3-D ROI to derive quantitative and/or semi-quantitative parameters from DCE-MRI for the differential diagnosis of breast lesions [19, 25]. Using a 3-D ROI, volumetric parameters can be obtained from the whole tumour. As regards tumour heterogeneity, volumetric parameters would more truly reflect the physiological characteristics of lesions in theory compared with using a two-dimensional ROI (2-D ROI) [26]. Previously, malignant breast tumours were found to have higher K^{trans} than benign tumours by using 3-D ROIs [19]. This is consistent with our
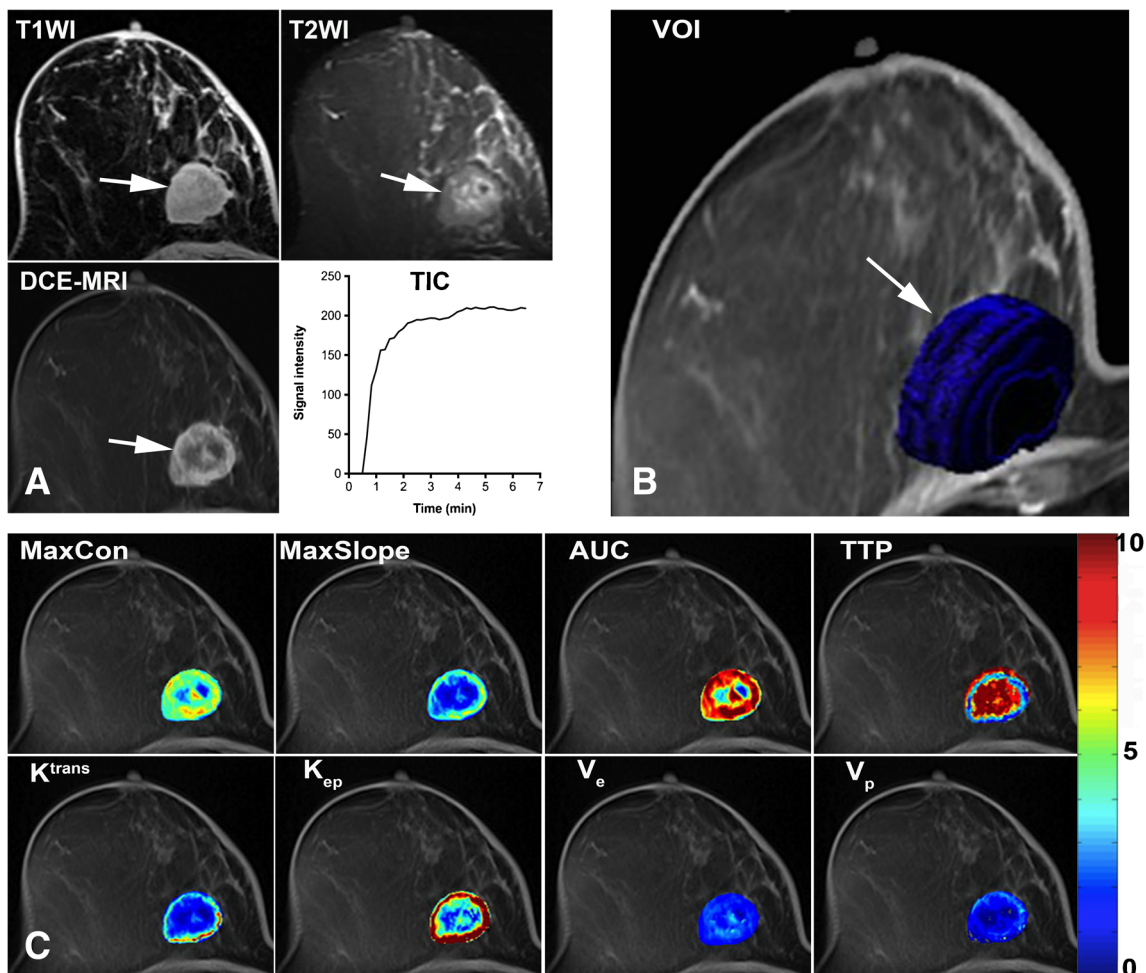
Fig. 2 Malignant breast tumour. (**A**) A 63-year-old woman has an infiltrating ductal carcinoma in the right breast, which is seen as a 36-mm mass (arrows) with isointense signal on T1WI and hyperintense signal on fat-suppressed T2WI, with a spiculated margin and rim enhancement on DCE-MRI (2 min after contrast injection) and a time-signal intensity curve (TIC) of type II; (**B**) DCE-MRI parameters are evaluated by a 3-D volume of interest (arrow); (**C**) Pseudo-colorized maps show individual parameters derived from DCE-MRI. This tumour has high MaxCon (0.1814), MaxSlope (0.4188), AUC (0.8897), K^{trans} (0.2112 min^{-1}), K_{ep} (1.3795 min^{-1}), V_e (0.1595) and V_p (0.0283), but low TTP (2.1685 min)

study results. However, it was also found that K^{trans} was significantly higher in benign breast tumours compared to malignant tumours [25]. This discrepancy might be related to the different temporal resolution of DCE-MRI. It was reported that 12 sec or higher temporal resolution is desired to avoid bias and allow for accurate qDCE-MRI parameters calculation [28]. The temporal resolution of DCE-MRI in our study was 8 sec, which is higher than that in the above two studies, which was 15-20 sec [19, 25].

A multitude of semi-quantitative parameters calculated from the time-signal intensity curve derived from DCE-MRI were previously investigated to determine the nature of tumours [6, 9]. Compared with semi-quantitative parameters, quantitative parameters have the advantage to be less sensitive to the MR machine set-up and data acquisition protocols, which makes inter-patient and inter-system comparisons more accurate [27, 28]. Our study showed that

AUC, MaxCon, TTP and MaxSlope had a higher sensitivity (81.0%-87.6%), specificity (77.4%-90.3%) and accuracy (80.1%-86.8%) for the differentiation of malignant from benign breast lesions than previously reported [6, 29]. However, the diagnostic accuracy of semi-quantitative parameters was lower than that of quantitative parameters, in particular, K^{trans} and K_{ep}. Quantitative parameters can improve diagnostic accuracy and provide an insight into the underlying biological characteristics of breast lesions [30, 31]. Previous studies showed that K^{trans} and K_{ep} could discriminate between malignant and benign breast lesions [18–20]. Our results showed that K^{trans}, K_{ep} combined with MaxSlope achieved a high diagnostic accuracy of 94.9%, which was higher than if each individual parameter would be used. This is reasonable because K^{trans} and MaxSlope represents a wash-in process of contrast agent in the tumour and K_{ep} represents a wash-out process [19].

Table 2 ROC analyses of morphological parameters, TIC type and qDCE-MRI parameters significant for discrimination between malignant and benign breast lesions (n=136)

Parameters	Cutoff value	AUROC (95% CI)	Sensitivity (95% CI)	Specificity (95% CI)	PPV (95% CI)	NPV (95% CI)	Accuracy (95% CI)
Size(mm)	9.5	0.794(0.696-0.893)	0.857(0.7333-0.9547)	0.667 (0.5005- 0.8517)	0.849(0.7852-0.9120)	0.765(0.5582-0.9676)	0.838(0.7752-0.8994)
Margin	2	0.779(0.690-0.867)	0.933(0.2840-0.9800)	0.452(0.3551-1.0000)	0.852(0.7866-0.9183)	0.667(0.4581-0.8473)	0.824(0.7559-0.8881)
Enhancement	2	0.695(0.587-0.803)	0.895(0.2100-0.9460)	0.419(0.0972-0.6679)	0.839(0.7753-0.9326)	0.542(0.3539-0.6314)	0.787(0.7148-0.8431)
TIC type	2	0.861(0.784-0.938)	0.981(0.4720-1.000)	0.581(0.2668-0.7968)	0.888(0.8311-0.9445)	0.900(0.7333-1.0000)	0.890(0.8381-0.9418)
K^{trans} (min^{-1})	0.053	0.949(0.913- 0.984)	0.876(0.7949-0.9637)	0.935(0.8380-1.000)	0.979(0.9468-1.0000)	0.690(0.5487-0.8300)	0.890(0.8356-0.9441)
K_{ep} (min^{-1})	0.514	0.954(0.920-0.987)	0.867(0.7091-1.0000)	0.903(0.7500-1.000)	0.968(0.9271-1.0000)	0.667(0.5244-0.8057)	0.875(0.8195-0.9309)
V_p	0.003	0.871(0.804-0.938)	0.895(0.5470-0.9640)	0.742(0.5001-0.8917)	0.921(0.8674-0.9728)	0.765(0.5598-0.9808)	0.838(0.7787-0.8963)
TTP (min)	4.787	0.922(0.876-0.968)	0.819(0.5470-0.9640)	0.903(0.7780-1.0000)	0.966(0.9184-1.0000)	0.596(0.4538-0.7313)	0.838(0.7734-0.9014)
MaxCon	0.110	0.812(0.719-0.905)	0.810(0.6971-0.9097)	0.774(0.6107-0.9198)	0.924(0.8689-0.9791)	0.545(0.4009-0.6947)	0.801(0.7369-0.8643)
MaxSlope	0.158	0.932(0.887-0.978)	0.876(0.7845-0.9887)	0.871(0.7248-0.9542)	0.958(0.9167-0.9998)	0.659(0.5095-0.8033)	0.868(0.8095-0.9236)
AUC	0.497	0.843(0.758-0.928)	0.857(0.7537-0.9548)	0.774(0.6040-0.9194)	0.928(0.8746-0.9808)	0.615(0.4691-0.7667)	0.838(0.7770-0.9002)

TIC time-signal intensity curve; *AUROC* area under the receiver operating characteristic curve; *CI* confidence interval; *PPV* positive predictive value; *NPV* negative predictive value. Margin: smooth=1, irregular=2, speculated=3. Enhancement: homogeneous=1, heterogeneous=2, rim=3. TIC type: Type I=1, Type II=2, Type III=3

K^{trans} is determined by microvascular blood flow, vessel permeability and vessel density [22], while K_{ep} represents vessel permeability. V_p was positively correlated with microvessel density [32]; V_e was influenced by cellular density and tumour interstitium [33]. In general, malignant breast lesions have higher microvascular blood flow, microvessel density, vessel permeability, cell density, contractible extracellular space and increased interstitial fluid pressure than a benign one. In our study, K^{trans}, K_{ep} and V_p were higher in malignant than benign breast lesions. These findings are consistent with previous reports [18, 19]. However, there was no difference in V_e. This reason might be assumed by the fact that cell proliferation in benign tumours may be active in some period, which would cause high cellular density and contractible tumour intersitium resulting in low V_e [34, 35].

Clinically, lesion morphology and kinetic TIC from DCE-MRI are regularly used to characterise breast lesions. In our study, the lesion size, margin and TIC were found to be independent predictors for malignancy. The diagnostic accuracy of lesion size, margin and TIC combined together was 89.0%, which was lower than that of quantitative parameters including K^{trans}, K_{ep}, and MaxSlope. Furthermore, the incorporating of morphology and TIC into qDCE parameters improved the diagnostic accuracy from 94.9% to 95.6%. Only a marginal benefit was observed for the incorporation of morphology and TIC. These results indicate that quantitative parameters are more important than morphological aspects including regular kinetic analysis of the lesions.

Notably, an underestimated T1 value from T1 mapping can cause the final overestimation of K^{trans} [28]. It has been reported that the dual flip angle method of T1 mapping results in errors in K^{trans} measurements compared to the multiple flip angle method; therefore, we chose to use a multiple flip angle to ensure correct derivation of K^{trans} value [36]. Moreover, we found that V_p has a high diagnostic performance with a higher sensitivity and specificity than reported previously [20]. In that study, however, a much lower temporal resolution of 56 sec was applied to acquire DCE-MRI data, which might have caused the underestimation of its performance [20]. It has been suggested to use a temporal resolution up to 8 sec, after which the errors grow rapidly with the decrease of temporal resolution [37]. To estimate well the V_p, a temporal resolution of 4 sec was recommended for the tracer kinetics model, which is mathematically identical to the Extended Tofts-Kety model [38]. Whereas, a trade-off should then be reached between temporal resolution and spatial resolution. In our study, we used a 3-D fast scanning sequence to ensure appropriate spatial resolution and high temporal resolution of 8 sec. Such temporal resolution is already higher than that used in similar studies on breast tumours [19, 20, 39].

There are several limitations in our study. First, our study population includes several types of malignant and benign breast lesions. To determine the diagnostic value of qDCE-
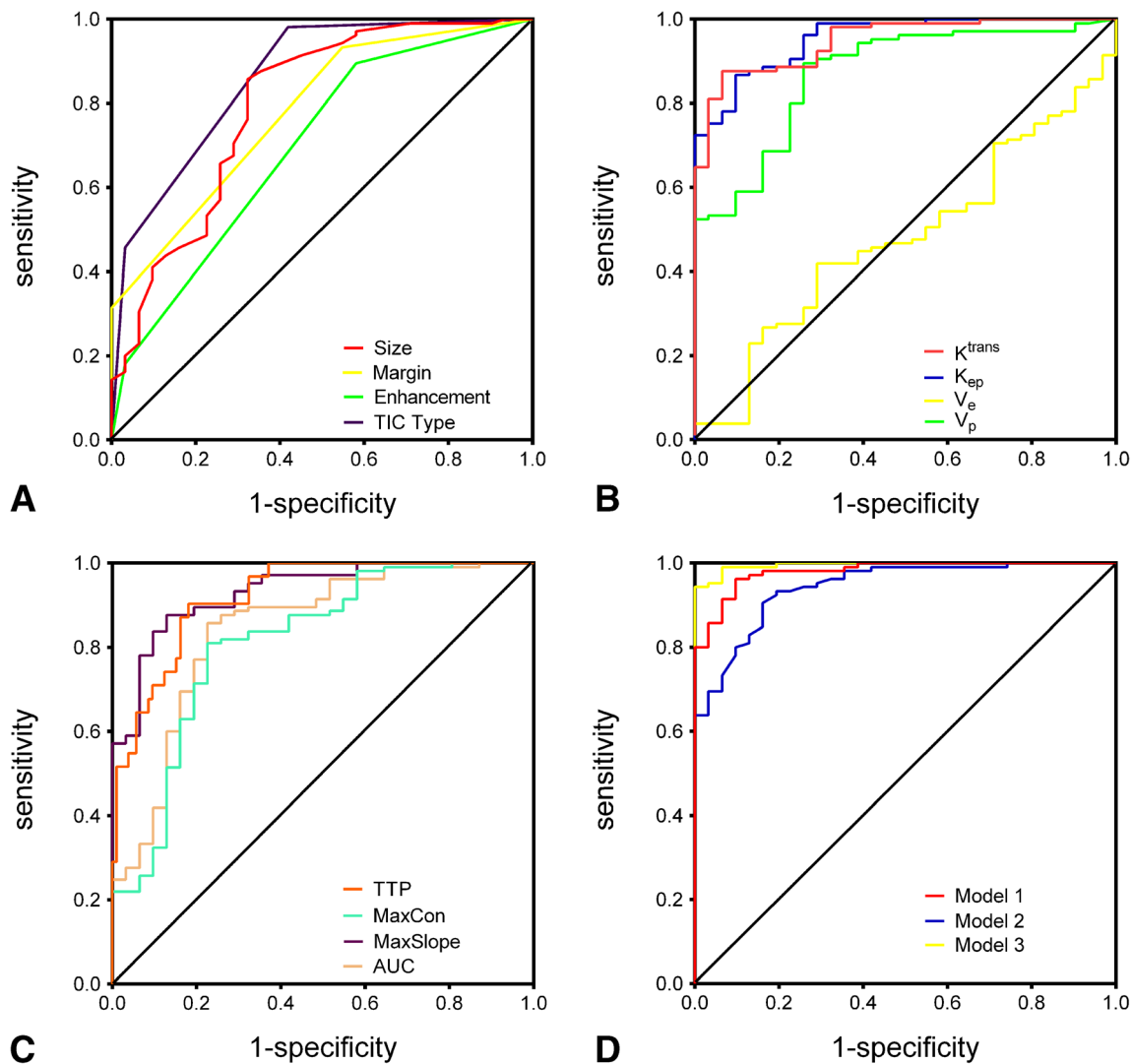
Fig. 3 Graph shows the ROC curves of morphological parameters, time-signal intensity (TIC) type (A), qDCE-MRI semi-quantitative (B) and quantitative parameters C), and the three models established by multivariate logistic regression (D) for differentiation between malignant and benign breast lesions. The AUROC, sensitivity, specificity, PPV, NPV and accuracy are listed in Table 3

MRI, we simply categorised them as two groups; malignant versus benign tumours. A previous report suggested that pharmacokinetic parameters are continuous variables, and cut-off values that match a binary classification of malignant versus

benign are unlikely [19]. Other reports demonstrated that pharmacokinetic parameters did not differ in different immunohistochemical subtypes of breast cancer [31, 40, 41]. Future studies with a larger number and a different subtype of breast

Table 3 ROC analyses of the three models established by logistic multiunivariate binary logistic analysis

Model	AUROC (95% CI)	Sensitivity (95% CI)	Specificity (95% CI)	PPV (95% CI)	NPV (95% CI)	Accuracy (95% CI)
Model 1	0.980 (0.961-1.000)	0.962 (0.925-0.999)	0.903 (0.801-0.100)	0.971 (0.918-0.994)	0.875 (0.710-0.965)	0.949 (0.911-0.986)
Model 2	0.943	0.905	0.839	0.950	0.722	0.890
	(0.904-0.983)	(0.832-0.953)	(0.663-0.946)	(0.887-0.984)	(0.548-0.858)	(0.838-0.941)
Model 3	0.995	0.943	0.100	0.100	0.838	0.956
	(0.989-1.002)	(0.880-0.979)	(0.888-0.100)	(0.963-0.100)	(0.680-0.938)	(0.923-0.989)

Model 1, qDCE parameters were chosen; Model 2, morphological parameters and kinetic curve type were chosen; Model 3, qDCE parameters, morphological parameters and kinetic curve type were combined together. AUROC area under the receiver operating characteristic curve; CI confidence interval; PPV positive predictive value; NPV negative predictive value

tumours should be warranted to verify the value of qDCE-MRI in the differential diagnosis of breast lesions. Second, only mass lesions were investigated. Mass lesions can be easily defined when a volumetric ROI is applied for evaluation of qDCE parameters. Future investigations are needed to determine whether this method could be used on non-mass enhancement lesions.

Conclusion

In summary, qDCE-MRI parameters have a good performance in differentiating malignant from benign breast lesions, in particular, K^{trans}, K_{ep} and MaxSlope. The qDCE-MRI parameters combined with morphological parameters and kinetic curve types could achieve a high diagnostic accuracy. The qDCE-MRI can be used as an important tool for preoperative differential diagnosis between malignant and benign breast lesions.

Compliance with ethical standards

Guarantor   The scientific guarantor of this publication is Jun Shen.

Conflict of interest   The authors of this manuscript declare no relationships with any companies, whose products or services may be related to the subject matter of the article.

Statistics and biometry   No complex statistical methods were necessary for this paper.

Informed consent   Written informed consent was obtained from all subjects (patients) in this study.

Ethical approval   Institutional Review Board approval was obtained from the institutional review board of Sun Yat-Sen Memorial Hospital of Sun Yat-Sen University (Guangzhou, China).

Methodology
• Prospective
• Diagnostic study
• Performed at one institution

References

1. Lin Y, Wang C, Zhong Y et al (2013) Striking life events associated with primary breast cancer susceptibility in women: a meta-analysis study. J Exp Clin Cancer Res 32:53

2. Morrow M, Waters J, Morris E (2011) MRI for breast cancer screening, diagnosis, and treatment. Lancet 378:1804–1811

3. Kul S, Cansu A, Alhan E, Dinc H, Gunes G, Reis A (2011) Contribution of diffusion-weighted imaging to dynamic contrast-enhanced MRI in the characterization of breast tumors. AJR Am J Roentgenol 196:210–217

4. Pereira FP, Martins G, Figueiredo E et al (2009) Assessment of breast lesions with diffusion-weighted MRI: comparing the use of different b values. AJR Am J Roentgenol 193:1030–1035

5. Bedrosian I, Mick R, Orel SG et al (2003) Changes in the surgical management of patients with breast carcinoma based on preoperative magnetic resonance imaging. Cancer 98:468–473

6. Yin J, Yang J, Han L, Guo Q, Zhang W (2015) Quantitative discrimination between invasive ductal carcinomas and benign lesions based on semi-automatic analysis of time intensity curves from breast dynamic contrast enhanced MRI. J Exp Clin Cancer Res 34:24

7. Kuhl CK, Mielcareck P, Klaschik S et al (1999) Dynamic breast MR imaging: are signal intensity time course data useful for differential diagnosis of enhancing lesions? Radiology 211:101–110

8. Ikeda DM, Hylton NM, Kinkel K et al (1999) Development, standardization, and testing of a lexicon for reporting contrast-enhanced breast magnetic resonance imaging studies. J Magn Reson Imaging 13:889–895

9. Heller SL, Moy L, Lavianlivi S et al (2013) Differentiation of malignant and benign breast lesions using magnetization transfer imaging and dynamic contrast-enhanced MRI. J Magn Reson Imaging 37:138–145

10. Bisdas S, Seitz O, Middendorp M et al (2010) An exploratory pilot study into the association between microcirculatory parameters derived by MRI-based pharmacokinetic analysis and glucose utilization estimated by PET-CT imaging in head and neck cancer. Eur Radiol 20:2358–2366

11. Thomas AA, Arevalo-Perez J, Kaley T et al (2015) Dynamic contrast enhanced T1 MRI perfusion differentiates pseudoprogression from recurrent glioblastoma. J Neuro-Oncol 125:183–190

12. Lee FK, King AD, Ma BB, Yeung DK et al (2012) Dynamic contrast enhancement magnetic resonance imaging (DCE-MRI) for differential diagnosis in head and neck cancers. Eur J Radiol 81: 784–788

13. Kamrava M, Sepahdari AR, Leu K et al (2015) Quantitative multiparametric MRI in uveal melanoma: increased tumor permeability may predict monosomy 3. Neuroradiology 57:833–840

14. Buadu LD, Murakami J, Murayama S et al (1996) Breast lesions: correlation of contrast medium enhancement patterns on MR images with histopathologic findings and tumor angiogenesis. Radiology 200:639–649

15. Flickinger FW, Allison JD, Sherry RM, Wright JC (1993) Differentiation of benign from malignant breast masses by time-intensity evaluation of contrast enhanced MRI. Magn Reson Imaging 11:617–620

16. Jansen SA, Fan X, Karczmar GS, Abe H, Schmidt RA, Newstead GM (2008) Differentiation between benign and malignant breast lesions detected by bilateral dynamic contrast-enhanced MRI: a sensitivity and specificity study. Magn Reson Med 59:747–754

17. Barnes SL, Whisenant JG, Xia L, Yankeelov TE (2014) Techniques and applications of dynamic contrast enhanced magnetic resonance imaging in cancer. Conf Proc IEEE Eng Med Biol Soc 2014:4264–4267

18. Li L, Wang K, Sun X et al (2015) Parameters of dynamic contrast-enhanced MRI as imaging markers for angiogenesis and proliferation in human breast cancer. Med Sci Monit 21:376–382

19. El Khouli RH, Macura KJ, Kamel IR, Jacobs MA, Bluemke DA (2011) 3-T dynamic contrast-enhanced MRI of the breast: pharmacokinetic parameters versus conventional kinetic curve analysis. AJR Am J Roentgenol 197:1498–1505

20. Fusco R, Sansone M, Filice S et al (2015) Integration of DCE-MRI and DW-MRI Quantitative Parameters for Breast Lesion Classification. Biomed Res Int. https://doi.org/10.1155/2015/237863

21. Fram EK, Herfkens RJ, Johnson GA et al (1987) Rapid calculation of T1 using variable flip angle gradient refocused imaging. Magn Reson Imaging 5:201–208

22. Tofts PS, Brix G, Buckley DL et al (1999) Estimating kinetic parameters from dynamic contrast-enhanced T(1)-weighted MRI of a diffusable tracer: standardized quantities and symbols. J Magn Reson Imaging 10:223–232

23. Tofts PS (1997) Modeling tracer kinetics in dynamic Gd-DTPA MR imaging. J Magn Reson Imaging 7:91–101

24. Tofts PS, Berkowitz B, Schnall MD (1995) Quantitative analysis of dynamic Gd-DTPA enhancement in breast tumors using a permeability model. Magn Reson Med 33:564–568

25. Chang YC, Huang YH, Huang CS, Chang PK, Chen JH, Chang RF (2012) Classification of breast mass lesions using model-based analysis of the characteristic kinetic curve derived from fuzzy c-means clustering. Magn Reson Imaging 30:312–322

26. Kim JH, Ko ES, Lim Y et al (2017) Breast Cancer Heterogeneity: MR Imaging Texture Analysis and Survival Outcomes. Radiology 282:665–675

27. Noworolski SM, Fischbein NJ, Kaplan MJ et al (2003) Challenges in dynamic contrast-enhanced MRI imaging of cervical lymph nodes to detect metastatic disease. J Magn Reson Imaging 17:455–462

28. Khalifa F, Soliman A, El-Baz A et al (2014) Models and methods for analyzing DCE-MRI: a review. Med Phys 41:124301

29. Di Giovanni P, Azlan CA, Ahearn TS, Semple SI, Gilbert FJ, Redpath TW (2010) The accuracy of pharmacokinetic parameter measurement in DCE-MRI of the breast at 3 T. Phys Med Biol 55:121–132

30. Oshida K, Nagashima T, Ueda T et al (2005) Pharmacokinetic analysis of ductal carcinoma in situ of the breast using dynamic MR mammography. Eur Radiol 15:1353–1360

31. Kim JY, Kim SH, Kim YJ et al (2015) Enhancement parameters on dynamic contrast enhanced breast MRI: do they correlate with prognostic factors and subtypes of breast cancers? Magn Reson Imaging 33:72–80

32. Van Dijke CF, Brasch RC, Roberts TP et al (1996) Mammary carcinoma model: correlation of macromolecular contrast-enhanced MR imaging characterizations of tumor microvasculature and histologic capillary density. Radiology 198:813–818

33. Turetschek K, Roberts TP, Floyd E et al (2001) Tumor microvascular characterization using ultrasmall superparamagnetic iron oxide particles (USPIO) in an experimental breast cancer model. J Magn Reson Imaging 13:882–888

34. Barnes SL, Quarles CC, Yankeelov TE (2014) Modeling the effect of intra-voxel diffusion of contrast agent on the quantitative analysis of dynamic contrast enhanced magnetic resonance imaging. PLoS One 9:e108726

35. Mills SJ, Soh C, Rose CJ et al (2010) Candidate biomarkers of extravascular extracellular space: a direct comparison of apparent diffusion coefficient and dynamic contrast-enhanced MR imaging–derived measurement of the volume of the extravascular extracellular space in glioblastoma multiforme. AJNR Am J Neuroradiol 31:549–553

36. Yuan J, Chow SK, Yeung DK, Ahuja AT, King AD (2010) Quantitative evaluation of dual-flip-angle T1 mapping on DCE-MRI kinetic parameter estimation in head and neck. Quant Imaging Med Surg 2:245–253

37. Schabel MC, Fluckiger JU, DiBella EV (2010) A model-constrained Monte Carlo method for blind arterial input function estimation in dynamic contrast-enhanced MRI: I. Simulations. Phys Med Biol 55:4783–4806

38. Henderson E, Rutt BK, Lee TY (1998) Temporal sampling requirements for the tracer kinetics modeling of breast disease. Magn Reson Imaging 16:1057–1073

39. An YS, Kang DK, Jung YS, Han S, Kim TH (1998) Tumor metabolism and perfusion ratio assessed by 18F-FDG PET/CT and DCE-MRI in breast cancer patients: Correlation with tumor subtype and histologic prognostic factors. Eur J Radiol 84:1365–1370

40. Koo HR, Cho N, Song IC et al (2012) Correlation of perfusion parameters on dynamic contrast-enhanced MRI with prognostic factors and subtypes of breast cancers. J Magn Reson Imaging 36:145–151

41. Yi B, Kang DK, Yoon D et al (2014) Is there any correlation between model-based perfusion parameters and model-free parameters of time-signal intensity curve on dynamic contrast enhanced MRI in breast cancer patients? Eur Radiol 24:1089–1096